

CRATUS: MOLTEN SALT THERMAL ENERGY STORAGE

by

BENJAMIN PRATT

Submitted in partial fulfillment of the requirements for the degree of

Master of Science

Physics Department

Science & Technology Entrepreneurship Program (STEP)

CASE WESTERN RESERVE UNIVERSITY

August 2022

CASE WESTERN RESERVE UNIVERSITY

SCHOOL OF GRADUATE STUDIES

We hereby approve the thesis of

Benjamin Pratt

candidate for the degree of

Master of Science*.

Committee Chair

Edward Caner

Committee Member

Dr. Robert Brown

Committee Member

Dr. Benjamin Monreal

Date of Defense

May 13, 2022

*We also certify that written approval has been obtained for any proprietary material contained therein

Table of Contents

List of Tables	4
List of Figures	5
List of Abbreviations	6
Abstract	7
Introduction	8
An Increasingly Strained Electrical Grid	9
The American Electrical Grid.....	12
Current Energy Storage.....	13
Thermal Energy Storage.....	18
Cratus Thermal Energy Storage	19
Supercritical CO ₂ (sCO ₂).....	20
Pressure Ratio	21
Simple Closed-Loop Brayton Cycle	23
Recuperated Closed-Loop Brayton Cycle.....	25
Recuperated, Recompression, Closed-Loop Brayton Cycle	26
Physics of RRBC: Applied to ThermaBlox	28
Current Molten Salts.....	31
Enhanced Molten Salts	32
The ThermaBlox Design	35
Assumptions for ThermaBlox Calculation.....	36
ThermaBlox Calculation	37
Cratus' Commercialization Plan Overview	41
Beachhead Market: Industrial Waste Heat Recovery.....	41
Concentrated Solar Power (CSP) Systems	44
Target Markets: Grid Scale Storage and Molten Reactors	46
Timeline and Market Entry	48
Conclusion	50
Appendix	53
Appendix A – Electricity over/under generation on the U.S. electrical grid.....	53
Appendix B – Typical lithium-ion battery functionality	54
Appendix C – sensible vs. latent heat explanation	55
Appendix D – TRL levels for EMS	56
Bibliography	57

List of Tables

1. Molten Salt Thermodynamic Properties.....	32
--	----

List of Figures

1. California Hourly Electric Load Vs. Load Minus Solar and Wind Capacity.....	11
2. DOE Duck Curve Over Time.....	11
3. Simplified Pumped Storage Hydropower Diagram.....	13
4. Hydroelectric Generation Sites and Pumped Storage Hydropower Sites in The United States.....	14
5. Possible Pumped Storage Hydropower Sites in The United States.....	15
6. Supercritical CO2 Pressure Vs. Temperature Diagram.....	21
7. Recuperator Effectiveness Based on Recuperated Heat and Pressure Ratio.....	22
8. Net Engine Efficiency Vs. Compressor Pressure Ratio.....	23
9. Simple Closed Loop Brayton Cycle.....	24
10. Recuperated Closed-Loop Brayton.....	25
11. Recuperated, Recompression Closed-Loop Brayton Cycle.....	26
12. Supercritical CO2 Brayton Cycle by Sandia National Laboratory.....	30
13. Cratus Conceptual Design.....	36
14. Cratus' Beachhead Market Valuation.....	43
15. NASA TRL Diagram.....	48
16. Lithium-Ion battery.....	54
17. Sensible vs. Latent Heat.....	55

List of Abbreviations

1. CAES = Compressed Air Energy Storage
2. CSP = Concentrated Solar Power
3. DOE = Department of Energy
4. EMS = Enhanced Molten Salts
5. EPCM = Encapsulated Phase Change Material
6. FES = Flywheel Energy Storage
7. FLiBe = Typical eutectic mixture of 67-33 mol% LiF-BeF₂ (FLiBe).
8. FLiNaK = Typical eutectic mixture of 46.5-11.5-42.0 mol% LiF-NaF-KF (FLiNAK)
9. GWP = Global Warming Potential
10. HEX = Heat Exchanger
11. ID = inner diameter
12. MSTES = Molten Salt Thermal Energy Storage
13. OD = Outer Dimension
14. PSH = Pumped Storage Hydropower
15. RRBC = Recuperated, Recompression Brayton Cycle
16. RTE = Round Trip Efficiency
17. SBIR = Small Business Innovation Research
18. STTR = Small Business Technology Transfer
19. TES = Thermal Energy Storage

Cratus: Molten Salt Thermal Energy Storage

BENJAMIN PRATT

Abstract

The increasing adoption of renewable sources of electricity (i.e. wind and solar farms) is being driven by the demand for carbon neutral electricity production. Although zero carbon is emitted during electricity production, these renewable energy sources suffer from intermittency, which is a mismatch between the supply and demand of electricity of the grid. Renewable energy sources, such as wind and solar, produce their peak electricity at off-demand periods of the day. This strains the electrical grid as it risks over-generation in some locations as well as a need for quick ramping of the electrical load which is hard on electricity producing infrastructure. As a partial solution to intermittency, pumped storage hydropower (PSH) is the dominant form of grid-scale energy storage. PSH accounts for 95% of the U.S. grid-scale storage capacity, which amounts to 22.9 GW of capacity [1]. The EIA also estimates with all possible sites, the U.S. can double their PSH capacity [1]. However, much more than that is not feasible being constrained by the availability of locations suitable for PSH. As a result, other grid-scale energy storage options are in development. The main options include batteries, thermal energy storage, compressed air energy storage (CAES) and flywheels. However, these storage options are plagued by high cost per kWh prices, location specificity (ex. PSH, CAES) and/or low energy density. With these concerns in mind, Cratus LLC is developing a molten salt thermal energy storage option known as ThermaBlox, which is

location-independent, low-cost, and high-capacity (with the capability to scale).

ThermaBlox will play a significant role in intermittency reduction while enabling increased adoption rates of renewable energy.

Introduction

Globally, the average emissions per person have surpassed 1 million pounds of carbon dioxide equivalent (CO₂e) emissions over a typical lifetime [2]. Nearly all of the emissions attributed to individuals are due to fossil fuel use as a result of the production of inexpensive products, constant travel, and increasing electricity production. This has led to a current atmospheric carbon dioxide concentration in excess of 400 [3] ppm and steadily rising. With these concerning trends in mind, the response has been to move directly to renewable sources of electricity (e.g. solar, wind, hydroelectric) that utilize inexhaustible sources of energy that contribute little to the emission of global warming potential (GWP) gases.

This response has, unfortunately, increased the risk of large-scale blackouts in nations with high renewable energy adoption rates while potentially slowing the proliferation of clean technology to developing nations. With heavy investment in solar and wind farms, the supply and demand for electricity has fallen further out of balance as the electrical grid cannot adequately match input electricity to output use by consumers. This problem, known as intermittency, refers to the over or under generation of electricity when compared to consumer demand. The concern of intermittency and inadequate load leveling have been the most significant technical barriers for increasing reliance on renewable sources of electricity generation.

Current methods to alleviate these challenges include pumped storage hydropower, lithium-ion (Li-ion) batteries, compressed air energy storage (CAES), thermal energy storage (TES), and flywheel energy storage (FES). These methods also have their own major technical concerns that must be overcome for large scale adoption. Technical obstacles such as location specific storage for CAES, high intrinsic losses for FES, and the overall high capital expense per unit of capacity (applying most pointedly to lithium ion batteries) have hindered significant use since Li-ion battery storage for all of Texas' storage needs would amount to \$6 trillion (at \$426/installed kWh of storage) [4]. As the push for adoption of renewable energy increases in vigor, the concern of intermittency must be alleviated. Cratus's molten salt thermal energy storage (MSTES) system will play a critical role in reducing GWP gas emissions by storing excess electricity then deploying it when supply dips below demand. The MSTES system will provide a low cost per capacity approach to intermittency reduction while offering MW-scale storage in a modular, location-independent system. The addition of MSTES systems to the electrical grid will increase the grid-scale energy storage by approximately 10 GWh over the first 5-7 years of production.

An Increasingly Strained Electrical Grid

The U.S. electrical grid is becoming more and more strained as renewables are added to the grid without the ability to level the load, effectively matching supply of power with demand. Intermittency causes the mismatch in supply and demand while generating new concerns such as load ramping, which all combine to reduce the

reliability of the grid. The present solution to intermittency within renewable energy sources is to utilize energy storage systems that can store energy when not needed then release it to the grid when ramping and load leveling are required to balance the grid.

Building a national grid that only relies on renewable sources of energy, without considering how to account for intermittency, will result in frequent blackouts and will put the U.S. decarbonization goals at risk. Blackouts seen in both California and Texas over the past two years have been a combined result of increased reliance on renewables without the ability to match the supply of electricity to the demand of consumers [5]. The blackouts in California and Texas showed that renewables cannot be the only ingredient in a state's (or country's) clean energy portfolio because they cannot readily increase or decrease power output to match demand. In both California and Texas, the electrical grid experienced a significant reduction in generation capability when compared to the required demand [8]. Under generation typically triggers rolling blackouts that strategically cut power to areas the local grid services to avoid a complete blackout [9]. The grid will require energy storage capabilities to alleviate

intermittency concerns and provide ramping capabilities when required to sustain the current quality of life for U.S. citizens.

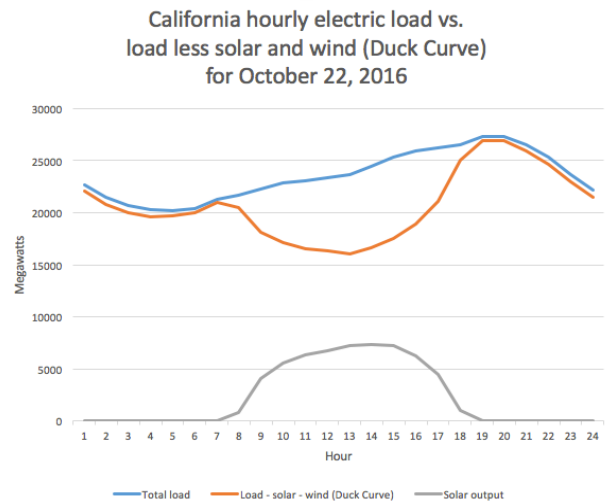


Figure 1. This figure shows the peak solar output period in California to be 1-3pm. At this time, the solar output (blue line) and the load minus solar and wind generation (orange line) begin to near each other. Should these paths cross overgeneration occurs [6].

Figure 2: The duck curve shows steep ramping needs and overgeneration risk

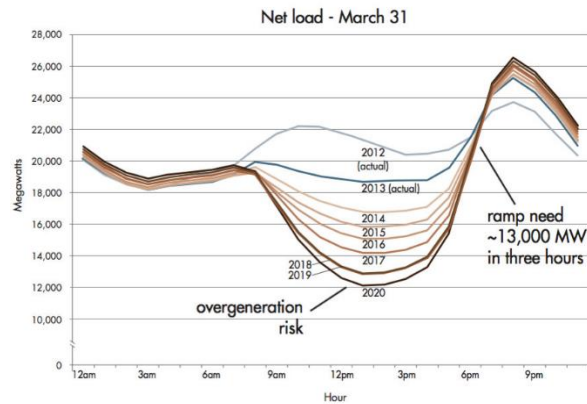


Figure 2. The duck curve shows two significant concerns with solar (and intermittent electricity sources). As time goes on, the decrease in required load may pose an overgeneration problem. The grid must also significantly ramp up electricity production which can cause issues with load leveling [7].

Furthermore, the solar “Duck Curve” threatens the stability of the electrical grid by requiring rapid ramping capabilities and potential overgeneration as renewables

continue to be connected to the grid. This curve, which is shown in both figures above, represents the potential for overgeneration to occur as well as a significant need to ramp up the total load on the grid in a small amount of time, which in this case was 13 GW in 3 hours. Seen in the figure to the right, net load (load minus solar generated electricity) has dropped lower and lower as time has passed. Additionally, the ramp up needed is a result of no solar generation after 5:30 pm – 6 pm, which additionally strains the power grid.

Ramping capabilities are alternatively referred to as dispatchable power generation. As the “Duck Curve” has been steepening over time, more dispatchable power will need to be connected to the grid to balance the load. These concerns bolster the argument for grid-scale energy storage and led to the DOE stating that “Solar coupled with storage technologies could alleviate, and possibly eliminate, the risk of over-generation.” This is because “curtailment isn’t necessary when excess energy can be stored for use during peak electricity demand” [7].

[The American Electrical Grid](#)

The U.S. electrical grid began operation in 1882 when Thomas Edison opened the country’s first power plant [10]. The plant served about 60 customers by generating electricity based on the demand of the customers. Although the grid now serves hundreds of millions of Americans, the methodology has largely gone unchanged. Electrical companies generate electricity based on the demand of their customers and they must balance supply versus demand to keep it running smoothly. Should too much

electricity be generated in relation to demand, grid infrastructure is at risk of significant damage (see Appendix A for explanation). Yet, if electricity generation is less than demand, blackouts occur. Although seemingly precarious, this balancing act has largely been successful for well over a century. Now, however, the balancing act between electrical supply and demand is much more difficult to manage as wind and solar farms intermittently produce power for the grid.

[Current Energy Storage](#)

The current grid-scale energy storage solution in the United States is pumped storage hydropower, which accounts for 95% of the U.S [11] grid-scale storage capacity (22.9 GW). Other forms of energy storage currently used tend to take the form of batteries, compressed air storage, current thermal energy storage, and flywheels. The present concern with energy storage systems is the high economic cost and the lack of scalability. Additionally, compressed air storage and pumped hydroelectric are geographically dependent while flywheels are unrealistic for grid-scale storage (ideal for smaller applications like data centers and hospitals).

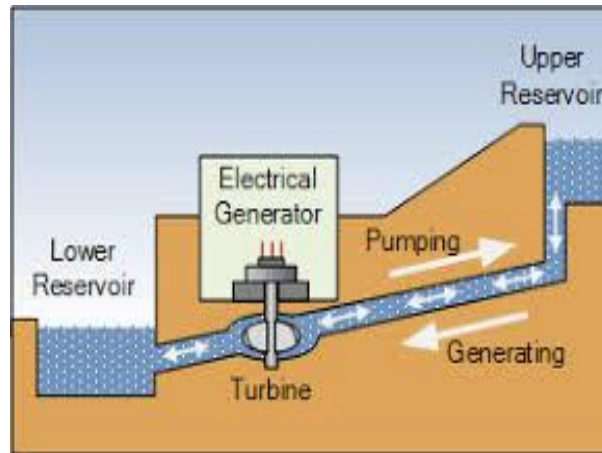
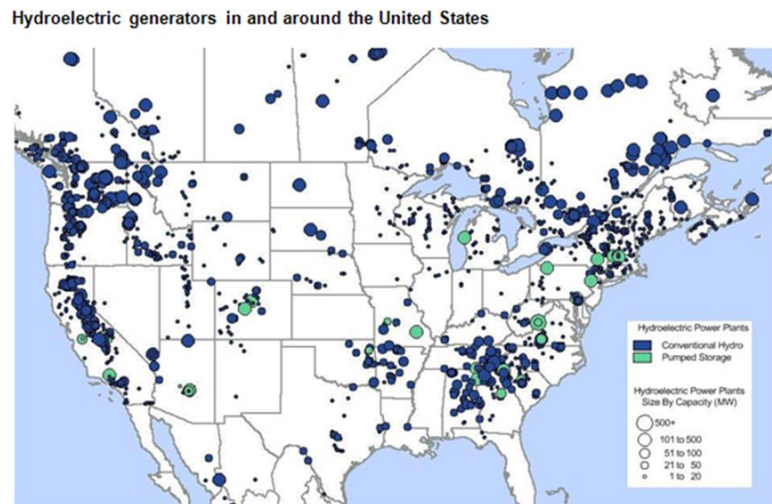


Figure 3. The lower reservoir holds water until electricity is incident on the generator. The generator spins the turbine and pumps water to the upper reservoir until needed. Once needed (typically when the intermittent electricity source isn't producing) the turbine is allowed to spin and generate electricity as water flows downhill from the upper to lower reservoir [12].

Pumped storage hydropower is the main form of grid-scale energy storage both in the U.S. as well as the rest of the world. It is the only commercialized grid-scale storage method due to a high round trip efficiency of 70-85% [13], and relatively low cost compared to other mediums (~17 cents/kWh vs. 42 cents/kWh for batteries) [14]. A typical PSH site has two separate basins of water. One basin is at a higher elevation than the lower one while the lower basin can be a standing body of water (closed loop PSH) or integrated into a flowing body of water (open loop PSH). Incident electricity, which usually is sourced from solar or wind farms, powers turbines located at the bottom basin which pump water up to the upper basin. This water is stored at the top until periods of electricity demand that outstrip the supply coming from renewable sources. At that point, water flows back down and spins the turbine(s) to generate electricity for

use. As mentioned above, PSH accounts for 95% of the United States' total grid-scale storage capacity.

However, this capacity is located most on the West Coast, the Northeast, and the Central Southeast of the U.S. These areas have already built out most of their hydroelectric capacity and are nearing the capacity for PSH. Other areas of the U.S. that do not have much PSH capacity aren't typically suitable for hydroelectric dams or PSH



Source: U.S. Energy Information Administration, derived from Energy Velocity

Figure 4. Diagram of all conventional hydropower plants in the United States as well as all PSH plants located in the U.S. The hydropower plants and PSH plants are concentrated on the West Coast, the Northeast, and Southeast [15].

such as Ohio, Texas, and Florida. These states do also have political considerations to take into account when discussing renewable energy, but as shown below, they do not have a significant number of available sites for PSH.



Figure 5. Possible projected PSH sites in the U.S. and Canada. Note the absence of many available sites in the middle of the U.S. as well as the states listed above (Ohio, Florida, Texas). This figure is from a report released in 2019 by Professor Andrew Blakers and other researchers with Australian National University's RE100 Group [16].

The predominant battery used for grid-scale energy storage is the Li-ion battery. Li-ion batteries use an electrochemical process to store energy when charged and release that energy by reversing the process to discharge (full explanation in Appendix B). This approach to energy storage is excellent for small (single consumer use) to medium use (local grids) because of the battery's high round trip efficiency, easy application, portability, and abundance of battery packs on the consumer market. Tesla Megapacks are the most well-known lithium-ion battery on the market for kWh-scale capacity. They typically come in a 3 MWh capacity while costing \$330 per installed kWh [17]. Additionally, Li-ion batteries tend to have a serviceable lifetime of 8-15 years¹ but do benefit from an excellent round trip efficiency² (RTE) of ~95% [18]. These metrics are

¹ Tesla's Megapack comes with a 15-year energy retention warranty. Projecting from that, Tesla expects their battery packs to last 15-20 years (on average).

² RTE = total output energy when fully discharged / total system capacity at full charge. A 95% RTE means 95% of input energy can be discharged and only 5% of the input energy is lost due to sources such as internal resistance, thermal losses, and electrochemical degradation.

unrealistic for grid scale energy storage, but typically serve the small-scale consumer market quite well when the objective is to provide battery backup for a home. Lithium-ion batteries are unrealistic for grid scale use based on an extremely high kWh cost when compared to PSH with Li-ion batteries being 2-6X more expensive than PSH (\$106/installed kWh vs. \$380-580/installed kWh) [14].

Compressed air energy storage (CAES) was initially developed to relieve intermittency due to renewable energy sources such as solar and wind, however, CAES has yet to be commercialized. The approaches to CAES largely revolve around how the heat generated, due to compression, is handled. CAES works by compressing air into a sealed container (often an underground salt cavern or drill site). Then once there is demand for energy the air is allowed to expand out of its container and spin a turbine to generate electricity. However, the act of compressing air increases its temperature and would cause compression to become less and less efficient as more energy would be required to compress the air if the heat was not dissipated. The only two commercial CAES plants in the world are both diabatic plants which means the heat generated as the air is compressed is later released as waste heat. This release of heat is a significant efficiency cost and reduced the overall perceived Return on Investment (ROI) of future plants. The ideal CAES plant is one that is adiabatic. Known as adiabatic CAES, these theorized plants function without the loss of thermal energy (adiabatic) by storing the waste heat until the air is released to spin a turbine. The heat is then transferred back to the air to increase efficiency. This method has yet to be commercialized since there has not been a good way to store and transfer the heat back to the air.

The highest efficiency approach typically utilizes a near-isothermal process (no change in temperature) while the lowest efficiency approach is to reheat the gas upon expansion with a natural gas combustion system. The current approach to CAES is to compress the air in a cavern and then vent the heat created upon compression. When energy is needed, the system allows the air to expand to spin a turbine. However, a significant inefficiency is present in this design because the air must be heated to expand which requires the CAES operators to expend energy to heat the air. Storage for the air also comes in many forms with the most common (noted above) being underground caverns since there is minimal insulation and sealing required while offering a massive volume for air storage. Typically, the RTE of CAES is between 50-60% efficient [19].

Thermal Energy Storage

Current TES systems represent an energy dense, high efficiency approach to energy storage and intermittency reduction with unfortunate economic shortcomings that have delayed serious commercialization. First, energy enters the TES system typically in the form of thermal energy via heated solar salts. The solar salt enters a heat exchanger to transfer the thermal energy from the external source to the internal working fluid of the TES. The internal heat fluid remains in its own insulated container until energy is desired. Once demand for electricity increases, the hot fluid is pumped through another heat exchanger that transfers heat to a working fluid (typically steam) which then goes through the steam Rankine Cycle to spin a turbine and generate electricity. These systems are typically very expensive and additionally suffer from a low

efficiency of 35-40% [20]. The cost per kWh of current thermal energy storage systems such as Abengoa's Concentrated Solar Power (CSP) and TES systems are very difficult to ascertain given the subsidies built into the pricing as well as protection of trade secrets, but the total system seems to be 20-40 cents per kWh [21][22].

Flywheels store energy by converting input electrical energy into kinetic energy in order to store electricity for later use with a typical storage capacity in the range of seconds to minutes of power [23]. Flywheels are typically used at data centers and similar installations that cannot tolerate an interruption of electricity. They function by taking input electricity to spin a dense cylinder of material to high speed on low friction bearings to function as a kinetic battery. They benefit from near instantaneous discharge rates but suffer from high cost, a comparatively lower RTE than Li-ion batteries of ~80% efficiency, and impractical scalability [24]. However, flywheels dominate niche markets where the continuity of power is critical to functionality. They are typically used in scenarios and situations that require instantaneous discharge of electricity to maintain the electricity to supply vital systems such as data centers and hospitals. In these scenarios they function as an Uninterruptable Power Supply (UPS) [23].

Cratus Thermal Energy Storage

Cratus thermal energy storage combines enhanced molten salts with a supercritical CO₂ (sCO₂) Brayton cycle, that is optimized based on pressure ratio and recuperator effectiveness, to achieve 50-55% round trip efficiency (RTE) from thermal

energy to electrical energy, a three times higher energy density, and at half the OPEX³ cost of current steam Rankine TES systems. Cratus' approach to thermal energy storage is known as the ThermaBlox. The ThermaBlox is a modular, scalable, inexpensive energy storage system for applications in both thermal energy storage and recycling, as well as electrical energy storage for future use. The specific Brayton cycle employed by ThermaBlox is known as a recuperated, recompression, closed-loop Brayton cycle (RCBC), which recycles waste heat and increases overall efficiency as a result.

Supercritical CO₂ (sCO₂)

Supercritical CO₂ is the most widely used supercritical fluid due to its excellent properties as well as low cost and abundance. Supercritical fluids are fluids that are held above both their critical pressure and critical temperature that combines the properties of gases and liquids. sCO₂ is chemically inert while being both non-toxic and non-flammable. The inexpensive nature of sCO₂ comes both from the abundance of the fluid as well as the ease of attaining supercriticality. The critical temperature of CO₂ is a mere 31 C, while the critical pressure is 74 bar (hydrogen is stored at 350-700 bar for reference)⁴ [25]. At this point, known as the critical point, reducing the temperature below the critical temperature results in a liquid while reducing the pressure results in a gas. Both of those scenarios experienced by the fluid are known as subcritical states. Supercritical fluids are unique in the fact that they expand to fill their container yet have

³ Operating Expenses = the day to day cost of operation and related expenses to run the system.

⁴ Atmospheric pressure is approx. 1.013 bar

a density similar to liquids. This attribute allows the turbine to generate electricity from the supercritical fluid flow by utilizing isentropic expansion to spin the turbine blades.

Pressure Ratio

The pressure ratio within a Brayton Cycle is the ratio between the minimum pressure and the maximum pressure within the system. Pressure ratio is typically the

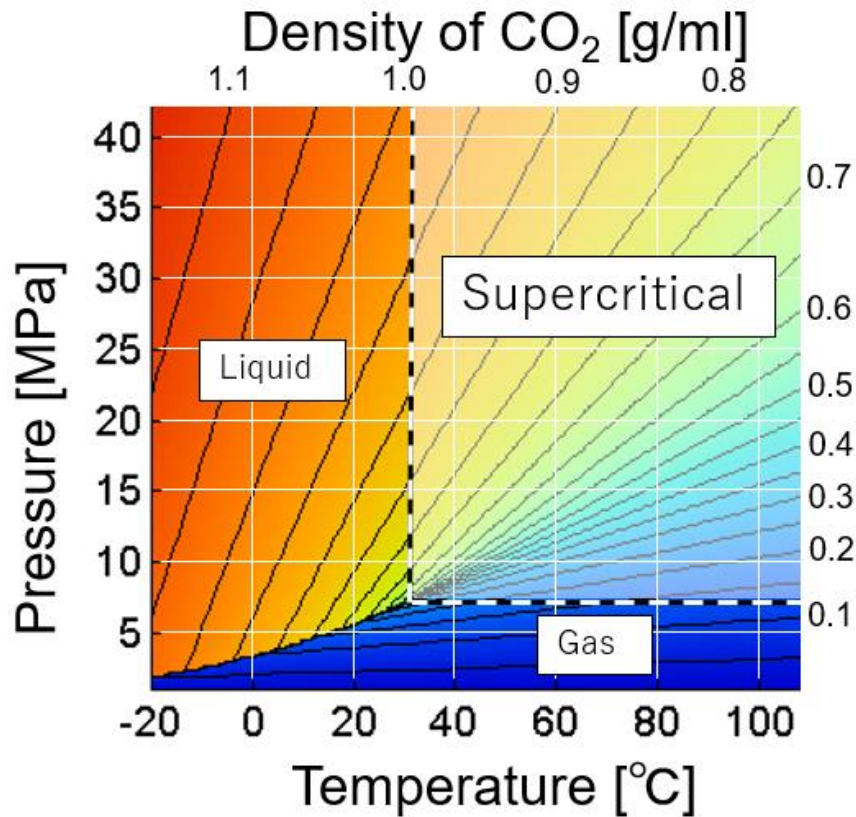


Figure 6. Subcritical fluids are held outside of the lighter “supercritical” zone in the figure. These subcritical fluids are either held below their critical pressure (the horizontal dashed line) or below their critical temperature (the vertical dashed line) [25].

most direct way to improve thermal efficiency of the cycle but increasing the ratio too

high will have an adverse impact on thermal efficiency of the system. Thermal efficiency as a function of pressure ratio is defined by the equation below [26].

Thermal efficiency is a function of pressure ratio defined by the above equation where η is thermal efficiency, PR is the pressure ratio, and k is equivalent to the specific heat of the fluid at the constant pressure (C_p) divided by the specific heat of the fluid at constant volume (C_v). This equation shows the direct connection between increasing PR and increasing η_{th} . This equation, does however, have limits in explaining the overall efficiency of a Brayton Cycle in its entirety. The thermal efficiency equation does not account for any compressors used and cannot properly educate an ideal design using compressors and recuperators.

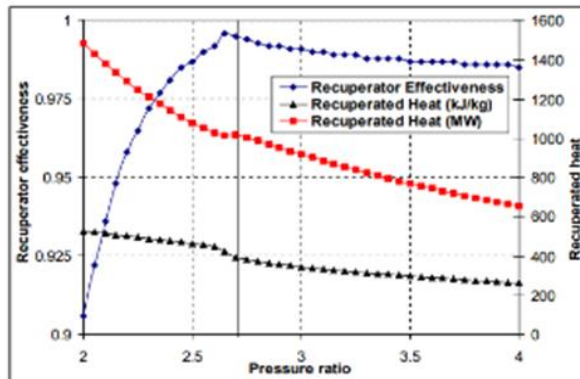


Figure 4.7 Recuperator parameters vs. the pressure ratio

Figure 7. The blue dotted line seen to peak around a 2.7 pressure ratio is the measure of recuperator efficiency as a function of pressure ratio. The relationship is clear that recuperator effectiveness rapidly increases from a 2-2.7 pressure ratio and reduces at a gradual pace after the peak [27].

The above recuperator effectiveness curves show how PR must be optimized in order to achieve the highest possible efficiency. Analyzing the above graphs, recuperator effectiveness is the same measure as recuperator efficiency. It is the

measure of actual energy transferred when compared to the total theoretical energy transfer possible.

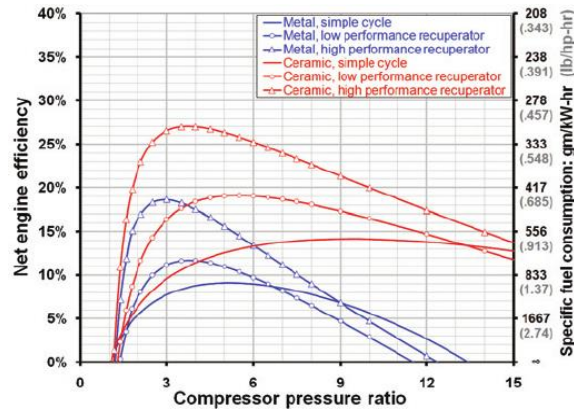


Figure 8. This figure shows the difference in optimal pressure ratio based on the level of performance as well as materials used in the Brayton Cycle design [27].

Simple Closed-Loop Brayton Cycle

Before explaining the recuperated, recompression, closed-loop cycle, it is necessary to understand the simple sCO₂ Brayton cycle. Before the fluid is heated within the system, it is compressed by the compressor seen in the upper righthand portion of the figure. The heater then transfers heat from the molten salts (or other working fluid) to the sCO₂, which is the working fluid of the Brayton cycle. The heater essentially functions as a heat exchanger (HEX) by transferring heat from the molten salt to the sCO₂. The (compressed) sCO₂ then functions similar to steam in a steam turbine to rotate the turbine. The spinning turbine is coupled with magnets, that when rotated,

induce an electrical current for output use. A small amount of the electricity generated by the turbine is transferred to the compressor to power it during use.

The heated sCO₂ that exits the turbine, after generating electricity, enters the gas cooler to release exhaust heat in order to lower the temperature of the fluid,

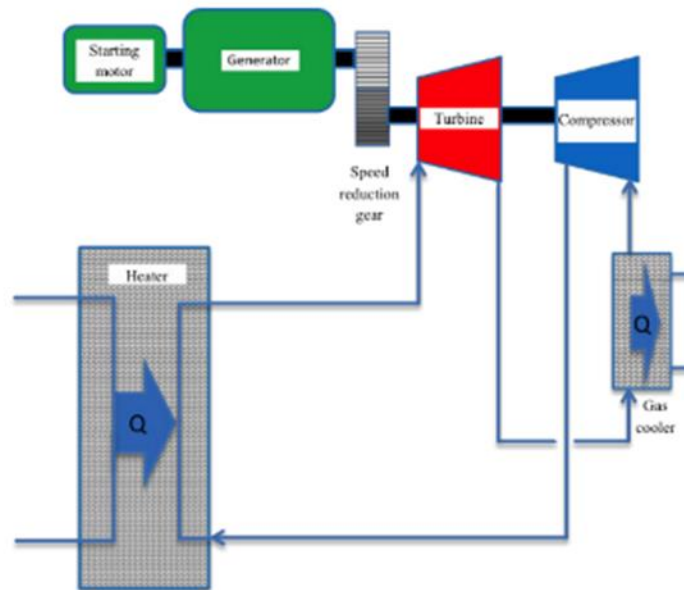


Figure 9. Simple Closed Loop Brayton Cycle. This Brayton loop utilizes incident heat from the heater to increase the operating temperature of the fluid which spins the turbine (red) to generate electricity [28].

typically by 50-150 C, before it enters the compressor [29]. Exhaust heat is released through the gas cooler because the compressor operates at its highest efficiency when the gas is cooled, and thus, easier to compress. Lower temperature gas is less energy intensive to compress than hotter gas because cooler gas requires a lower pressure (when held at constant volume) to increase the temperature due to the ideal gas law. [30]. Due to compression, the fluid has marginally increased in temperature prior to entering the heater to further be heated to 700 C.

Recuperated Closed-Loop Brayton Cycle

The addition of a recuperator to better utilize internal heat, is employed in the recuperated closed loop cycle to decrease the amount of thermal exhaust from the gas cooler, effectively increasing overall efficiency. Within the cycle, the sCO₂ transfers through the recuperator, which is cooled by the outlet sCO₂ from the compressor. The reduced heat of the sCO₂ prior to the gas heater, improves efficiency by retaining more thermal energy within the system and releasing less heat from the gas cooler. The cycle then functions the same as the simple cycle with the addition of the outlet sCO₂ fluid absorbing heat from the outlet turbine fluid via the recuperator.

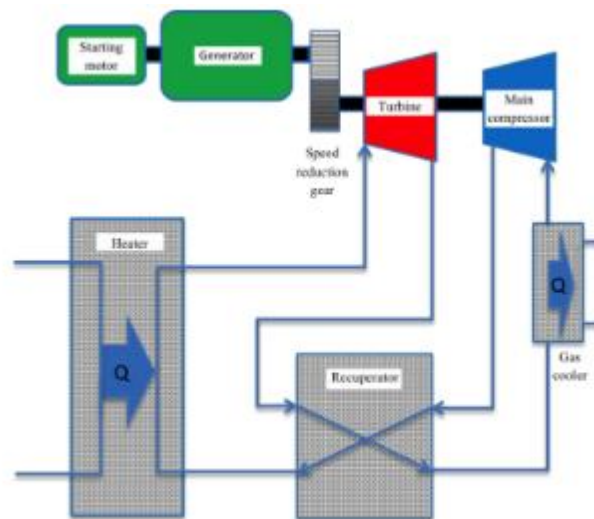


Figure 10. Recuperated Closed-Loop Brayton Cycle. This Brayton loop utilizes incident heat from the heater to increase the operating temperature of the fluid which spins the turbine (red) to generate electricity. This system has the addition of a recuperator to decrease thermal losses from the gas cooler [28].

Recuperated, Recompression, Closed-Loop Brayton Cycle

Finally, the Brayton Cycle utilized by Cratus is the RRBC. This cycle currently achieves approximately 55% efficiency with sCO₂ as the working fluid. The RRBC utilizes two temperature recuperators, a low temperature and high temperatures recuperator, along with two compressors to optimize the internal heat utilization while cutting down on thermal exhaust from the gas cooler.

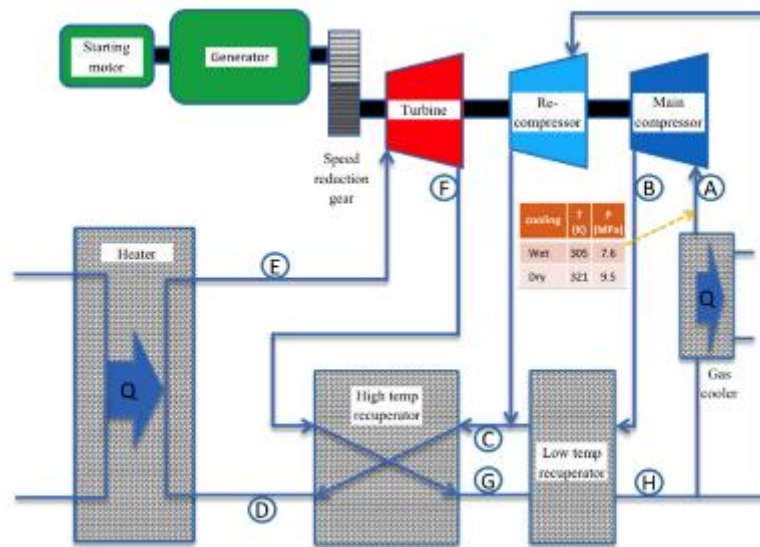


Figure 11. Recuperated, Recompression, Closed-Loop Brayton Cycle. This style of Brayton Cycle is the most thermodynamically efficient being able to achieve 55% efficiency based on employing two recuperators and two compressors to reduce thermal losses and required compression energy [28].

In the RRBC approach, cooled gas from the gas cooler enters the main compressor (A). The main compressor uses a portion of the electricity generated by the turbine to compress the cooled gas. The compression of the gas increases the overall energy within the system (enthalpy) and increases the energy flow rate within the system since the fluid is denser. The compressed gas then enters the low-temperature

recuperator (B) where it increases in temperature from a cross flow of higher temperature sCO₂. This increased sCO₂ then travels to the high-temp recuperator (C) where the same heating process occurs. This heating process reduces the heat losses of the system by transferring thermal energy from the hotter fluid to the cooler fluid, thus, reducing the thermal energy vented from the cooler. At point D, the heated supercritical fluid enters the heater. The heater, in Cratus' situation, transfers heat from the molten salt loop to the fluid which carries the increased thermal energy to the turbine (E). At this point, the turbine is spun using the expanding supercritical fluid. The expanding fluid does work on the turbine, effectively converting thermal energy to physical work that can generate electricity. The majority of the produced electricity is transferred out of the system to be used for other purposes, but a small portion is diverted to power the two compressors within the system. As the gas exits the turbine and enters the high temp recuperator (F), the high temperature fluid transfers energy from itself to the lower temperature fluid (reducing thermal losses in the system). Point G shows the travel of the reduced heat fluid that enters the low temp recuperator and again reduces thermal losses of the system by transferring heat from the higher temperature fluid to the low temperature fluid. Finally, the cooled fluid from the low temp recuperator outlet is split 60/40 (H) with 60% of the fluid entering the gas cooler and 40% bypassing the cooler and traveling to the re-compressor. The reason for the split is to reduce the amount of energy lost in the system, however, the exact percentages are dependent upon system design, materials used, and the thermodynamics of the fluid.

Physics of RRBC: Applied to ThermaBlox

The performance of ThermaBlox depends on the thermodynamic properties of the Enhanced Molten Salts (EMS), the physical design, and how the internal components are manufactured and operate. ThermaBlox utilizes next generation Encapsulated Phase Change Material (EPCM) that increases the thermal conductivity of the salts as well as triples the heat capacity. This results in a footprint that is 1/3 that of Cratus' competitors with the same performance. Finally, assuming industry standard materials and dimensions are kept constant, ThermaBlox is expected to require two independent EMS loops to hold 8 MWh of thermal energy based on simplicity, manufacturing constraints, and the laws of Thermodynamics.

With an understanding of the recuperated, recompression, closed-loop Brayton cycle, the thermodynamics of the cycle are significantly easier to understand. The cycle starts with heat being transferred from the EMS to the fluids via simple conduction. The hot EMS enters the HEX at 720 C and conducts thermal energy to the supercritical CO₂. The sCO₂ enters the heat exchanger at approximately 500 C and is heated to 700 C before progressing to the turbine. The fluid, after entering the turbine, undergoes near-perfect isentropic expansion⁵ to transfer thermal energy from the fluid to electrical output energy. The transfer of energy occurs because the fluid rapidly expands once less confined in the turbine (compared to the pipe that transferred it there) which exerts pressure on the turbine blades. The turbine blades turn and induce a current in a wire

⁵ Perfect Isentropic expansion is an increase in the volume of a fluid that does not increase the entropy of the system. Practical isentropic expansion is expansion of a fluid with a small increase in entropy.

by creating a magnetic field from rotating magnets with the turbine blades. This process results in a reduction in temperature of the fluid because a portion of the energy within the fluid was transferred to electrical energy that is either used for external electrical use or to power the internal compressors. Interestingly, the entropy of the system does not change while undergoing isentropic expansion because the exiting energy is accompanied by a precipitous drop in temperature, which balances the minimal energy loss of the system.

After the sCO₂ exits the gas turbine at a reduced temperature, it interacts with the heat rejector which cools the fluid before it enters either the compressor or re-compressor. The fluid is generally cooled by wet cooling using something like water to act as a heat sink for the supercritical fluid. The active cooling method is utilized to increase the overall efficiency of the supercritical system. The heat exhaust significantly improves the overall efficiency of the system because the cooled gas requires significantly less energy to compress when compared to hotter fluids.

After exiting both compressors, the fluid stream undergoes isochoric heating to increase the temperature of the working fluid. An isochoric process is one in which the volume of the heated fluid is held constant as the amount of thermal energy in the system increases. This is done by transferring thermal energy from the comparatively hot sCO₂ stream to the colder stream of sCO₂ that is flowing in the opposite direction towards the compressors. The methodology of heat transfer within the recuperators is unknown, however, it seems probably that the same formula of enhanced molten salts

as a medium within the recuperators (not the exact same flow of salts)⁶ is used to transfer heat from the hotter flow of fluid to the cooler flow of fluid.

The decision to utilize the EMS as the heat transfer medium seems likely from a logistical perspective as well as a thermodynamic perspective. Compared to conventional molten salts, the EMS has higher thermal conductivity which would allow for higher efficiency of the system. As the commercialization of Cratus' ThermaBlox comes to mind, simplifying the logistics of materials needed would allow for easier fabrication due to requiring no new materials to function correctly.

Supercritical CO₂ Brayton Cycle

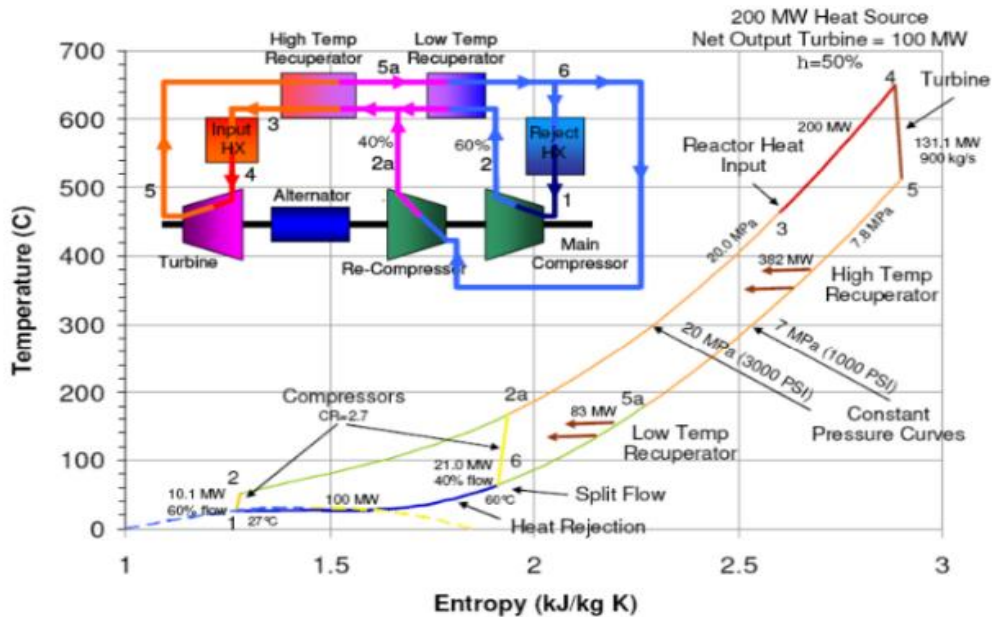


Figure 12. The Supercritical Brayton Cycle based on Sandia National Laboratory's design. This cycle is the recuperated, re-compression Brayton Cycle that employs two recuperators and two compressors [29].

⁶ The same formula of molten salt will likely be used because the components used to contain the heat transfer medium can be made of the same materials as all other components without expanding the technical requirements of the internal components. There has been recent interest in sand as a heat transfer medium so sand may be a low-cost alternative to EMS since it tends to have a higher thermal conductivity coefficient than EMS (about ~ 1 W/m K for EMS vs. ~ 2 W/m K for sand). This was not the focus of this paper and will require further research to determine sand's viability as a contained heat transfer medium for recuperators.

Current Molten Salts

The current molten salts used for CSP and TES systems either suffer from poor comparative thermodynamic properties, low cost-effectiveness, or high corrosion which have all lead to limitations in the commercialization efforts of TES and CSP systems. The most common molten salt used in CSP systems is a 60-40 binary combination of NaNO_3 / KNO_3 . This compound is stable up to 620 C and cost effective at \$0.5/kg [31]. Thermal conductivity has been difficult to experimentally determine but it is approximately 0.45-0.55 W/m C at 700 C [32]. The heat capacity NaNO_3 and KNO_3 as solar salt is measured to be 1500 J/kg C at 700 C according to researchers at the University of Alabama [33].

Conversely, FLiBe and FLiNaK fluoride molten salts⁷, often used in nuclear reactors, have similar thermodynamic qualities. FLiBe's specific heat capacity is measured at 2414.17 J/kg C (at 700 C) and a thermal conductivity coefficient of 1.0-1.1 W C/m [34]. Compared to FLiBe and the binary nitrate salt solution, FLiNaK's heat capacity is measured to be 1882.8 J/kg C at a maximum measured operating temperature of 650 C [34]. FLiNaK's thermal conductivity, according to the literature, averages 0.92 W/m K at its measured maximum operating temperature of 650 C. Currently there are no salts that can attain >700C and none that are low cost. All three fluids have low viscosities; however, solar salt (NaNO_3 / KNO_3) has the lowest viscosity of 0.0017 Pa*s followed by FLiNaK at 0.0029 Pa*s and FLiBe at 0.0056 Pa*s [35].

⁷ Typical eutectic mixture of FLiNaK is 46.5-11.5-42.0 mol% LiF-NaF-KF (FLiNAK) and 67-33 mol% LiF-BeF₂ (FLiBe). A Eutectic mixture is a mixture of substances whose melting point is lower than any of the constituent substances on their own.

Although the thermodynamic characteristics of the three fluids are extremely important, viscosity must also be taken into account due to the need for the molten salts to be pumped through the system. A lower viscosity reduces the cost of pumping within the molten salt system significantly and enables a lower cost of operation for CSP and thermal battery systems.

Molten Salt Thermodynamic Properties							
Material	cost [34]	thermal conductivity [35]	specific heat capacity [35]	viscosity [35]	Energy Density GJ/m ³ (700 C)	Density	Mass Energy Density (MJ/kg)
FLiBe	>\$2/kg	1.0 W/m K	2414.17 J/kg C	0.0056 Pa*s	3.28	2036 @ 500C, 1938 @700 C kg/m ³ [36]	1.69
FLiNaK	\$2.0/kg	0.92 W/m K	1882.8 J/kg C	0.0029 Pa*s	2.78	1998-2116 from 773-993K [37]	1.32
NaNO ₃ / KNO ₃	\$1.3/kg	0.55 W/m K	1500 J/kg C	0.0017 Pa*s	2.85	1840 @ 400C [34]	1.08

Table 1. This table compares the thermodynamic, physical, and economic qualities of the three most common molten salts used in CSP applications as well as planned modular molten salt reactors. NOTE: Viscosity is the measure of a liquid's resistance to flowing, lower viscosity equates to thinner, easier to pump liquid. There is no direct relationship between density and viscosity [34], [35], [36], [37].

Enhanced Molten Salts

Cratus' enhanced molten salts are a combination of conventional solar salts/molten salts already in use with the addition of micron scale capsules of encapsulated phase change material. The addition of encapsulated phase change material in molten salts is to increase the rate of heat flow into and out of the system as well as improve the heat capacity of the system to reduce the overall cost per kWh of stored energy.

Claimed in Cratus literature, their enhanced molten salts have three times (3X) the energy density of conventional molten salts which leads to higher ROI of TES projects and overall cost-effectiveness. The most likely route to tripling the energy

density of the EMS (functioning as the heat transfer fluid) would be due to tripling the heat capacity. This is the likeliest route to a higher energy. Encapsulated phase change material (EPCM) has been known for decades to be an ideal material for high energy density, high temperature applications [38]. This knowledge has largely emanated from the structure and performance of phase change materials. The typical EPCM is bead-like with an outer layer of material which has a higher melting point than the material's expected environment. The internal core, which is protected by the external coating/layer, has a lower melting point than the high end of the expected temperature range yet a solidification point higher than the low end of the temperature range.

These chosen thermal properties of the EPCM (in the core) enable the overall thermal system to take advantage of both “sensible heat” and “latent heat”⁸. Since the melting point of the EPCM is lower than the highest expected operating temperature, the EPCM will absorb thermal energy up to its melting point (known as sensible heat) and then absorb additional energy while transitioning from solid to liquid states by melting (known as latent heat). Conversely, when the absorbed heat is desired for external use, the EPCM travels through a heat exchanger whose operating temperature is below the solidification point of the EPCM. In this situation, known as the discharge cycle of the system/material, releases all of the heat that was recently absorbed through sensible and latent heating (see Appendix C for further description). The discharge cycle

⁸ Sensible heat is a change in temperature that does not involve changing phase and can be sensed such as a pot of water getting warmer prior to boiling. Latent heat is the thermal energy involved in a phase change (the heat transferred to water once it is at its boiling point).

is the thermodynamic opposite of the charging cycle (addition of heat to EPCM) by releasing additional heat from the transition back from liquid to solid.

Ideally, EPCMs require several parameter optimizations before their use in extreme environments such as molten salt baths. Firstly, EPCM capsules should be coated with enough material to maintain mechanical performance while undergoing thermal cycling, yet the coating must be thin enough to optimize thermal performance characteristics. Too thin of a shell will drastically reduce durability, but too thick of a protective shell will hamper thermal conductivity (storage and release capabilities) as well as reduce the overall thermal energy storage capacity.

Secondly, the external coating must be made of a material that has high thermal conductivity⁹ and is durable to thousands of thermal cycles before requiring a replacement. Third, the smaller the diameter of the total EPCM, the shorter solidification time of the EPCM. A shorter solidification time equates to a faster discharge rate which is ideal for thermal energy storage and heat transfer applications. Finally, the capsules of EPCM must have a high enough energy density to minimize the amount of required EPCM capsules needed within the conventional molten salts. Minimizing the volumetric concentration of EPCM capsules added to the heat transfer fluid improves viscosity which decreases pumping costs as well as lowers the material demands for pumping components. A lower volumetric concentration of EPCM

⁹ Seemingly intuitive, a high thermal conductivity improves the rate of heat flow from EPCM to heat transfer fluid (or vice versa) while a lower thermal conductivity reduces overall performance.

additionally improves the rate of convective heat transfer which compresses the rate of charge/discharge.

With all of the performance parameters known, the major obstacle impeding commercialization is long-term durability. There are several proposed EPCMs in the literature that are designed to be able to survive long periods of frequent thermal cycling while being pumped through a loop, however, there does not seem to be any instances of deployed EPCMs in molten salt loops. But, should Cratus be able to achieve the creation of long-term EPCM in extreme environments, their assertion of tripling the energy density of solar/molten salts may very well be an understatement.

[The ThermaBlox Design](#)

The ThermaBlox system is designed for input energy from a variety of sources. The first, and most obvious, is the input of thermal energy from a concentrated solar farm which transfers its thermal energy via solar molten salt. The second source is electrical to thermal energy conversion from an electric resistance heater used to convert electrical energy to thermal energy. Finally, the last option is thermal energy from nuclear fission. This heat can be upwards of 600 C in Generation 4 modular molten salt reactors.

Regardless of the medium, the internal thermodynamics remain the same; Thermal energy is transferred to the EMS, the EMS then transfer thermal energy to the sCO₂, and the sCO₂ loop creates electricity. In order to determine the expected output, the input energy must be calculated then reduced according to the internal efficiency of the ThermaBlox (50%). To calculate the required energy input, the temperatures of the EMS flow into and out of the initial heat exchanger must be considered. The inlet temperature is set at 520 C and the outlet temperature of the hot EMS is determined to be 720 C with both being set by the schematic given.

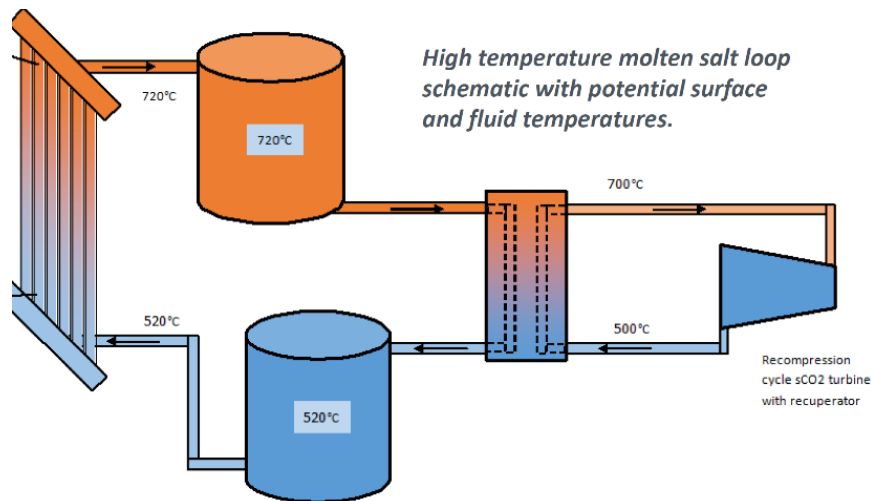


Figure 13. Cratus' conceptual design of ThermaBlox. The actual ThermaBlox design utilizes a baffled one-tank design that combines the 720 C and the 520 C tanks into a single tank. This decreases the overall footprint of the system and reduces pumping requirements [39].

Assumptions for ThermaBlox Calculation

ThermaBlox is stated to be rated for 4 Mega Watts of of output electricity (4 Mwe). If we assume a 50% round trip efficiency, the required input thermal energy is 8 Mega Watts (8 MWth). Additionally, for the internal dimensions, it is assumed each pipe that carries molten salt within the external and internal heat exchanger is 1.5 m long.

Since ThermaBlox is stated to fit in a 20-40 ft shipping container, the heat exchangers are taken to be 5 meters apart. This assumption provides a basis to calculate the thermal losses from imperfect insulation.

The assumptions for the materials, and their properties, are as follows.

Hastelloy-N, developed by Oak Ridge National Lab for use as a container for molten fluoride salts, is used for all piping and is the base alloy for the heat exchangers. The insulation around all piping is calcium silicate. The piping is assumed to have an inner diameter (ID) of 0.15 m and an outer diameter (OD) of 0.20 m. The ID of the insulation begins at the outer diameter of the piping, which is 0.20 m and the OD of the insulation is taken to be 0.31 m. The density of the EMS is taken to be 1.94 g/cm³ C (similar to commonly used molten salts), and its thermal conductivity is claimed to be 3X the thermal conductivity of FLiBe salts (2,373 J/kg C), amounting to 7,120 J/kg C. The mass flow rate of FLiBe salts is typically claimed to be 5 cm/s so Cratus' EMS are assumed to have the same mass flow rate.

[ThermaBlox Calculation](#)

In order to calculate the rate of heat flow into the system the specific heat formula is used.

$$Q = m * C * \Delta T$$

However, the equation lacks time dependence which is required should we compute the heat flow of the system. Dissecting the equation, the specific heat of the fluid "C" cannot have time dependence as it never changes. The " ΔT " also cannot change

because the fluid is constantly being heated from 520 C to 720 C. This leaves the first term of the equation “m”, which is the mass of the fluid within the system. However, since the heat flow rate is desired, the mass flow rate must be calculated to provide time dependence and account for the constant flow of the EMS.

$$\frac{dQ}{dT} = \frac{dm}{dt} * C * \Delta T$$

The mass flow rate is a separate equation that depends on the density, velocity, and cross-sectional area the fluid is traversing. The density and velocity of the EMS are proprietary, so both parameters will be assumed as the same as FLiBe salt’s parameters which are 1.94. The cross-sectional area is the area of a perpendicular plane within the Hastelloy-N pipe.

$$\frac{dm}{dt} = \rho * v * A$$

All terms are now known and the thermal energy flow in the system can be calculated. The below equation measures total heat flow into the system by taking into account the density of the working fluid “ρ”, the flow velocity of the working fluid within the system “v”, the cross-sectional area of the piping carrying the working fluid “A”, its specific heat capacity “C”, and the total change in temperature “ΔT”.

$$\frac{dQ}{dt} = \frac{dm}{dt} * C * \Delta T = \rho * v * A * C * \Delta T$$

The density of the EMS is taken as 1.94 g/cm³, the velocity of the EMS is 5 cm/s, the cross-sectional area of the Hastelloy-N pipe is calculated as 14.43 cm² (A = π * r²),

the specific heat of the EMS is approximately 7.12 kJ/kg * C (triple the C of FLiBe), and the change in temperature is 200 C based on the assumption that the inlet Ems is 520 C and the warmed outlet fluid is 720 C. With all parameters known based on assumptions made, the thermal energy flow into the system is approximately 200 kJ/s, or 200 kW.

$$\frac{dQ}{dt} = 1.94 \frac{g}{cm^3} * \frac{5cm}{second} * 14.43 cm^2 * \frac{7.12 kJ}{kg} * 200^o C = 199.34 \frac{kJ}{second}$$

This input is based on only using one pipe of ID = 0.15 m. Since the capacity of the system is claimed to be 8 MWth, the thermal energy flow must be increased to allow for proper output. The easiest solution to increase internal thermal energy flow within the system is to increase the ID of the internal piping to allow for more EMS to circulate or to increase the total number of pipes

Assuming material parameters and change in temperature will remain constant, the only modification available to increase input thermal energy flow is to increase the cross-sectional area of the pipe. This can be done either by increasing the total number of pipes within the system or increasing the ID of the single pipe. Given this system is expected to be fabricated as simply as possible, the ideal situation seems either to limit the number of pipes, or to use a larger number of small pipes within the system.

Analyzing it from manufacturers standpoint, it seems that a single pipe of a larger diameter is the best option for each of fabrication and system durability. This is largely due to the increase in cost as complexity of valves, pipes, and heat exchangers increase.

To achieve the expected 8 MW input of thermal energy, the cross-sectional area of the internal piping must be solved for in order to achieve the appropriate amount of EMS within the system.

$$\frac{\frac{dQ}{dt}}{\rho * v * C * \Delta T} = A$$

At this point, 8,000 kW (8 MW) will be substituted in for $\frac{dQ}{dt}$. Density, velocity, and change in temperature will be held constant. Therefore, the cross-sectional area of the internal piping can now be solved for. A is found to be 579.17 cm² which then leads to r being equivalent to 13.6 cm shown in the below equations.

$$A = \frac{8000 \text{ kW}}{1.94 \frac{\text{g}}{\text{cm}^3} * \frac{5\text{cm}}{\text{second}} * \frac{7.12 \text{ kJ}}{\text{kg}} * 200^\circ \text{ C}} = 579.17 \text{ cm}^2$$

$$A = \pi r^2 \rightarrow \sqrt{\frac{A}{\pi}} = r \rightarrow \sqrt{\frac{579.17 \text{ cm}^2}{\pi}} = 13.6 \text{ cm radius}$$

This also doesn't take into consideration that larger ID pipes also need to be greater thickness to handle the increased thermomechanical stress. Yet, the alternative would be to fabricate significantly more complex piping within the system to decrease thermomechanical stress. With such a large increase in cross-sectional surface area, it seems the design would be least complex (from a manufacturing standpoint) if there

were two independent salt loops as opposed to one large pipe. The radius of the internal pipe is 9.6 cm if there are two loops, but over 13.5 cm with a singular loop.

Cratus' Commercialization Plan Overview

Cratus plans to first enter the industrial waste heat recovery market because ThermaBlox will not require the sCO₂ loop if the goal is heat recycling. This will reduce the complexity of the path to market and generate early revenue. The generated revenue will attract external investment which will be used to fully develop the supercritical fluid loop and EMS. At the second stage, Cratus, along with its partners, will integrate ThermaBlox into concentrated solar power systems. This application will both prove the tandem functionality of the enhanced molten salts with the supercritical fluid loop as well as garner appropriate funding through major (\$10-30M) federal grants to construct a full-scale production facility for ThermaBlox to produce 100 ThermaBlox per year. At this point, Cratus will be in position to grow into its two main target markets of grid-scale energy storage and molten salt nuclear reactors. Market entry is projected as late 2026 into 2027 and will see the funding development of all necessary components to Technology Readiness Level (TRL) 3-7 prior to market entry.

[Beachhead Market: Industrial Waste Heat Recovery](#)

Cratus will initially target industrial waste heat recycling. Typical industrial heat operations, such as glass and steel manufacturing, can operate well over 1,000C. Steel production typically operates at temperatures exceeding 1,500C. The steel making

industry uses waste heat to heat on-site facilities or local buildings [40]. However, industrial heat recovery systems are immature at best, and cannot be directly recycled back into the initial application (i.e. steel production). Furthermore, industrial heat recovery systems perform even worse at temperatures higher than 400 C [41]. Consequently, the market sector is in need of heat recycling that will dramatically improve efficiency at high operating temperatures.

Cratus has targeted the industrial waste heat recovery market as a beachhead market because the application of Cratus' ThermaBlox, in this case, negates the need for the supercritical fluid cycle. In order to recover waste heat, ThermaBlox will receive thermal energy from either exhaust air or the molten steel at the external heat exchanger. The thermal energy will heat the enhanced molten salts of the system which will be circulated to the internal heat exchanger. Rather than transferring heat from the EMS to the supercritical fluid, the internal heat exchanger will transfer energy back into the production process. With minimal thermal losses in the system, thermal to thermal efficiency is at, or above, 95%.

The global steel product market was estimated to be \$1.01 trillion as of 2018 [42]. The North American steel product manufacturing market was worth \$36.4B in

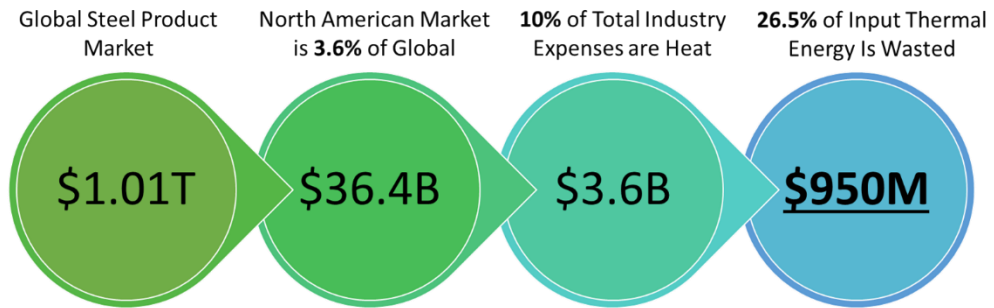


Figure 14. Cratus' beachhead market value of industrial waste heat in North America. The global steel product market is valued at \$1.01 trillion as of 2018 with the North American market accounting for 3.6% of the global market. Looking at the market, 10% of all expenses are tied to heat and 26.5% of that heat is wasted. Therefore, Cratus projects the North American industrial waste heat market to be \$950 million.

approximately 3.6% of the global market. In order to approximate the market value of high-grade waste heat in the steel product industry, it's helpful to know about 10% of the total cost to produce steel products is tied to thermal energy input [43].

Additionally, ~26.5% of all input heat is wasted [44]. Therefore, the total wasted capital per year in the North American steel product market is roughly \$950M.

Cratus first began its commercialization approach by applying for DOE SBIR/STTR funding. This process, if successful, tends to require the participation of industry partners as well as universities and national labs. Cratus began developing relationships with potential strategic partners by including them in SBIR/STTR awards where they worked alongside the Cratus team. Second, Cratus now both functions as the prime awardee on some awards while being the subrecipient on others as long as the award is with a strategic partner/institution and the technology is increasing in its TRL. This

process has enabled Cratus to leverage its relationships in the private and academic sectors to garner funding towards the creation of pilot project as well as exploring potential first customers. As a result, Cratus has found a first customer in the beachhead market given their dual expertise in fluid loop/thermal energy transfer technology and CSP power.

Cratus projects the pilot plant will require \$5 million in funding in order to demonstrate the concept to the point it creates interest for follow on funding. The \$5M will go towards pilot plant erection as well as increasing the technology and manufacturing readiness level of the enhanced molten salts to the point they can be produced in large enough quantities for pilot plant demonstration. Finally, once a successful demonstration of the pilot plant is verified, venture capital, private equity, and federal renewable energy grants will be courted for a final development of \$10-20M for full production of ThermaBlox units.

[Concentrated Solar Power \(CSP\) Systems](#)

Once Cratus has entered the industrial waste heat recovery market and begun generating revenue, they will use the generated revenue to garner additional external investment to finish development of the supercritical with their associated partners. At this point, once ThermaBlox is fully developed, Cratus will work with its partners to apply the ThermaBlox system to CSP systems. These systems currently heat molten solar salts with the magnified heat of the sun and generate steam through a steam Rankine cycle. Cratus will tie in ThermaBlox to transfer heat from the solar salts into the

ThermaBlox system for higher thermal to electrical energy conversion efficiency of ~55% compared to current TES systems being 30-40% efficient. The higher efficiency will be the result of a higher operating temperature (720 C vs. 560 C) and the use of the supercritical fluid loop.

The CSP application is the next application Cratus will target for the technical reasons explained above as well as the major investments, and the importance, the DOE has placed in CSP systems. Since 2018, the DOE has invested at least \$62 million in CSP technology with the trend expected to continue (if not increase) since the DOE's goals for CSP technology were achieved earlier than expected [45]. Due to the high level of funding being targeted at developing CSP systems, Cratus plans to use DOE funding to increase the TRL of the ThermaBlox system components to enable its compatibility with CSP systems. DOE funding will target the increase in TRL of the EMS and internal component TRL. The current EMS TRL is at level 2 with DOE funding projected to increase that level to TRL 4 (See EMS TRL explained in Appendix D). At a TRL 4, this EMS and the overall ThermaBlox design becomes much less risky and, as a result, more attractive to Venture Capital and Private Equity investments. The other portion of non-dilutive DOE funding will target the increase in TRL for internal components that are designed to combat the corrosion and high temperature. These components, and production methodology, is currently at a TRL 4 and will need to improve to TRL 5 which will demonstrate the components in molten salt loops at appropriate corrosion levels and temperatures.

The concentrated solar power market in North America is projected to be \$1.3 billion in 2023 and is expected to be growing at a very healthy 10-12% CAGR [46]. Additionally, high-temperature molten salts have a realistic ability to improve overall plant efficiency by 15-17% [46]. Finally, the expected installed GW capacity for CSP plants in 2023 is projected to be 2.47 GW and coming to a per GW of installed capacity cost of \$539.3M [46]. Therefore, if overall output is increased by 15% due to the use of high-temperature molten salts the market will increase in value by \$200M¹⁰. As a whole, the total installed thermal energy storage used in combination with CSP plants is projected to reach 630 GWh by 2023 [47].

Target Markets: Grid Scale Storage and Molten Reactors

ThermaBlox is being developed with the intention to provide a high efficiency energy conversion method for next generation modular molten salt reactors to help provide a safe source of dispatchable power. Cratus expects this emerging market will play a major role in the near future for American electricity generation. As a result, the small footprint and high efficiency of ThermaBlox will directly integrate into and complement modular molten salt nuclear reactors that are projecting to operate at or near 700 C. Additionally, Cratus' ThermaBlox will work alongside solar and wind farms to provide grid-scale energy storage. ThermaBlox will be utilized as grid-scale energy storage for intermittent renewable energy sources. This application will require

¹⁰ 2.47 GW * 0.15 * \$539M/GW = ~\$200M

resistively heating the enhanced molten salts of the thermal energy storage system by utilizing the incident electricity from the wind or solar farm.

The projected capturable modular molten salt reactor (MMSR) market in 2022 is projected to be \$3.8 billion, although a majority of the market is dominated by generation three¹¹ fission reactors [38]. Modular reactors are expected to play a major role in the pursuit of the United States' decarbonization goals due to a variety of factors. MMSR's are considered a generation 4 nuclear reactor meaning that it is currently being researched and has yet to be commercialized. However, the generation 4 name also carries with it expectations of increased safety (with many reactors being referred to as intrinsically safe) as well as higher system efficiencies and lower costs [48]. With a capturable market valuation of \$3.8 billion, there is only one operational generation 4 reactor (High-temp, gas-cooled, pebble bed reactor) located in China [49]. Therefore, there is a significant market available which will drive new technology and new development.

The global alternative energy storage market is projected to top \$5.67 billion in 2022, with the overall industry growing at an extremely high CAGR of 34%. Of the \$5.67 billion market, \$5.65 billion will be energy storage used in tandem with either wind or solar [50]. Renewable energy adoption and automotive electrification (adoption rates of EVs) will have significant influence on the alternative energy storage markets. Therefore,

¹¹ Generation 3 nuclear reactors were designed to have superior efficiency, durability, and safety when compared to generation 2 reactors. There has never been a nuclear accident with a generation 3 nuclear reactor, while both the Fukushima and Chernobyl accidents utilized generation 2 reactors.

Cratus intends to utilize ThermaBlox in tandem with solar generation to reduce intermittency of solar power as well as provide load leveling capabilities on the grid.

Timeline and Market Entry

Cratus ThermaBlox are projected to be ready for consumer purchase by late 2025 into 2026. However, before Cratus enters the industrial waste heat recovery market they expect to require \$5M for to develop and demonstrate a small-scale pilot plant. Once the pilot plant in operational, Cratus will seek out \$20-30M in venture funding to increase the scale of production, deploy units to the market, and integrate into developing CSP projects.

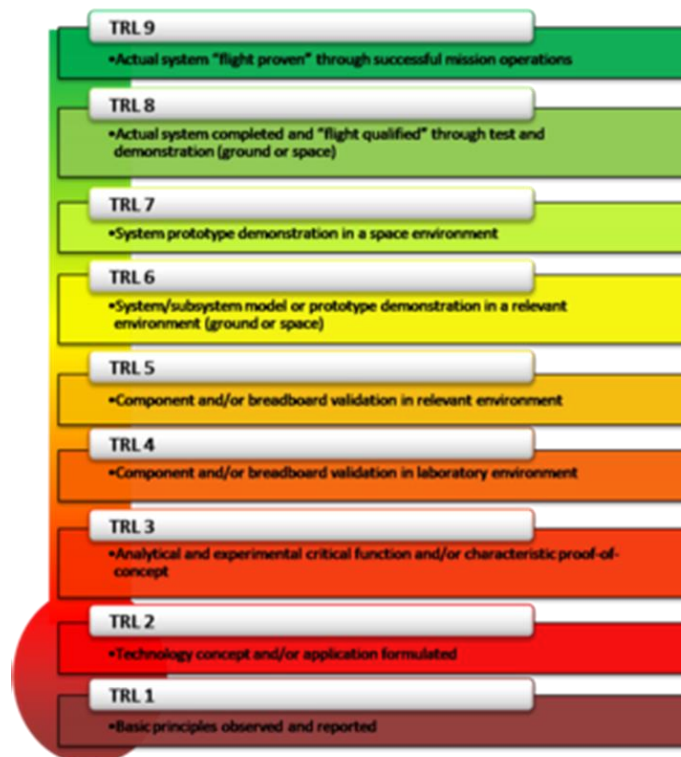


Figure 15. NASA TRL figure detailing levels of technology readiness from ideation to proven results in the intended application [51].

Cratus' strategy to raise \$5M over the next two years is expected to require several phases of fundraising as the technology improves. Cratus plans to raise \$1M in non-dilutive funding to raise the TRL of the enhanced molten salts to TRL 4/5¹², up from its current TRL 2. This improvement will both improve the technological feasibility of the project as well as de-risk the ThermaBlox project for future investors. Observing that the EMS is the least developed component of the project, raising the TRL will significantly raise the entire technology readiness level of the project. The non-dilutive funding will likely come in the form of a Department of Energy (DOE) phase II, Small Business Innovation Research grant (SBIR). These grants typically amount to \$1-1.6M and look highly upon projects with strong ties between industry and academia. An additional phase 2 award will fund the development of the molten salt heat exchangers. The molten salt HEXs are currently at a TRL 4 and will require \$500-750K to increase to TRL 7. Cratus expects to achieve TRL 7 with that level of funding because they already have significant partners in both academia and industry that can test the HEX in the intended environment of performance.

After proving technical feasibility of the EMS and HEX in their respective environments, the final \$3 million of the project will come from a short series A round of fund raising that will include private investment from industrial partners, clean energy

¹² TRL 6 is significant because it validates the material in its intended environment WITH acceptable performance. It is a major milestone for R&D. It is also in the "Valley of Death" (typically TRL 5,6,7) that suffers from poor funding because the technology is in between being proven and being investable.

venture firms, and private equity investors. At this stage, Cratus will utilize the \$3 million in funding to optimize the ThermaBlox design for small scale, pilot plant production.

With the total \$5 million investment and improved enhanced molten salts, Cratus will develop, and operate a small-scale pilot plant that will provide validation for the design.

Conclusion

The increasing adoption rates of renewable energy sources of electricity have begun to highlight flaws of the US electrical infrastructure that must be corrected in order to protect the United States' future decarbonization goals. Intermittency reduction is at the forefront of the conversation as solar and wind farms either under or over generate electricity throughout the day. As a result, the electrical grid is susceptible to blackouts that can cut power to millions of people, critical infrastructure, and cause chaos. The expected solution to intermittency is grid scale energy storage that can provide load-leveling capabilities.

The current issues and shortcomings of grid scale energy storage can be summarized as high cost per stored kWh, difficult to scale, low energy density, and/or low efficiency. With these shortcomings, grid-scale energy storage has yet to be deployed on any reasonable scale, and the concerns of intermittency have yet to be alleviated. With these concerns in mind, Cratus envisioned ThermaBlox. ThermaBlox storage energy at the lowest cost of the market at \$200/MWh as opposed to utility-scale lithium-ion battery storage and TES systems that are each approximately \$400/MWh [52]. Additionally, Cratus designed ThermaBlox with enhanced molten salts

which increase the energy density of the ThermaBlox system by ~3X when compared to current TES systems as well as currently partner with industry leaders in supercritical fluid loops to increase the overall efficiency and miniaturize the design. The miniaturization and consequent modularity of ThermaBlox will allow end users to scale their energy storage capacity as their need for capacity increases.

Cratus is commercializing ThermaBlox using the current Department of Energy push to accelerate the development of CSP power plants to fund R&D efforts. Cratus is targeting the development of its enhanced molten salts and internal materials as the main benefactors of funding. This strategy is designed to create salable products prior to market entry for ThermaBlox. The plan is to generate early revenue by selling enhanced molten salts and high temperature, corrosion resistant internal materials to CSP systems, TES systems, and next-generation modular molten salt reactors. Additionally, Cratus expects private investment from partners to develop and operate a pilot plant. This investment, and subsequent development will attract the final phase of \$15 million funding to see Cratus into market entry and fund the integration of ThermaBlox into CSP systems. Finally, after a market validated application, the expectation is Cratus will continue manufacturing and selling ThermaBlox or be acquired by a larger company in the renewable energy space.

With the development of CSP plants and modular molten salt reactors, there is realistic reason to believe a company in one of those markets will be the buyer of Cratus. Modular molten salt reactor companies are the most likely candidate for

acquisition because modular reactor technology is about a decade from market entry and Cratus' technology would cover 2/3 of the total reactor functionality. The internal fission and subsequent heat generation would still require separate designs, but the heat transfer out of the system and subsequent thermal to electrical energy conversion could be done using ThermaBlox technology.

Appendix

Appendix A – Electricity over/under generation on the U.S. electrical grid

When there is too much electricity produced on the grid, the overall frequency on the grid increases to account for the extra energy. Machines on the grid are rated for frequency ranges (with the ideal frequency in the U.S. being 50 Hz) and if the frequency goes beyond it, the substation or machinery will be disconnected from the grid. If they do not disconnect from the grid, the machines will overheat and burn which will cause irreparable damage. If the machines do disconnect, especially in a short amount of time, this can lead to a cascading effect that takes several plants or substations down all at once. This is typically called a blackout. It can happen in either scenario (over or underloading the grid, although most typical is overloading).

The larger concern, when under generation occurs, is typically the need to turn on “peaker plants” which are low efficiency natural gas plants but can generate power rapidly. These produce significantly more emissions than typical natural gas power plants and are extremely expensive both for plant operators and consumers in “time-of-day” pricing states/areas. The typical efficiency of “peaker plants” is approximately 30-40% based on their simplified design known as a simple cycle gas turbine. Conversely, typical natural gas power plants, which are used to generate a majority of electricity (sourced from fossil fuels), are combined cycle gas turbines that run at 60% (or more) efficiency [53].

Appendix B – Typical lithium-ion battery functionality

There are four main components of a lithium-ion battery: anode, cathode, separator, and external circuit. The anode is typically referred to as the negative terminal of the battery, while the cathode is the positive terminal. The separator keeps the anode and cathode separate and allows lithium ions to pass through. However, the electrons that are ejected from the lithium cannot pass through the separator and must pass through the external circuit to do electrical work and then recombine with the lithium ion.

When a lithium-ion battery is discharging (powering an external source), lithium ions move from the anode to the cathode by recombining with electrons. In recombining, the electrons must pass through the external circuit where they do electrical work that can be harnessed. Should the battery be charged, the process goes in reverse. The external energy ionizes the lithium at the cathode and the lithium ions pass through the separator to settle at the anode where they wait until the next discharge cycle.

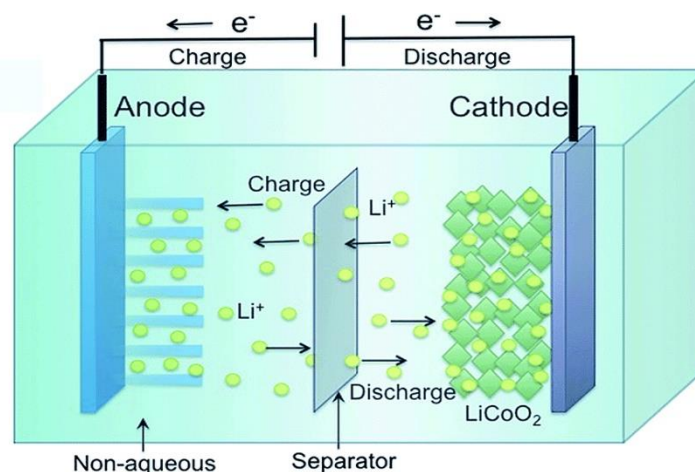


Figure 16. typical lithium-ion battery chemistry and functionality [54].

Appendix C – sensible vs. latent heat explanation

Sensible heat is the heat that can be measured by a thermometer. This heat heats up an object and can be felt. This form of heat is what would increase the temperature of water. Latent heat is the form of heat that, in the example of water, melts ice but does not increase the ice's temperature. Put another way, it is the heat that is added to a system during a phase change.

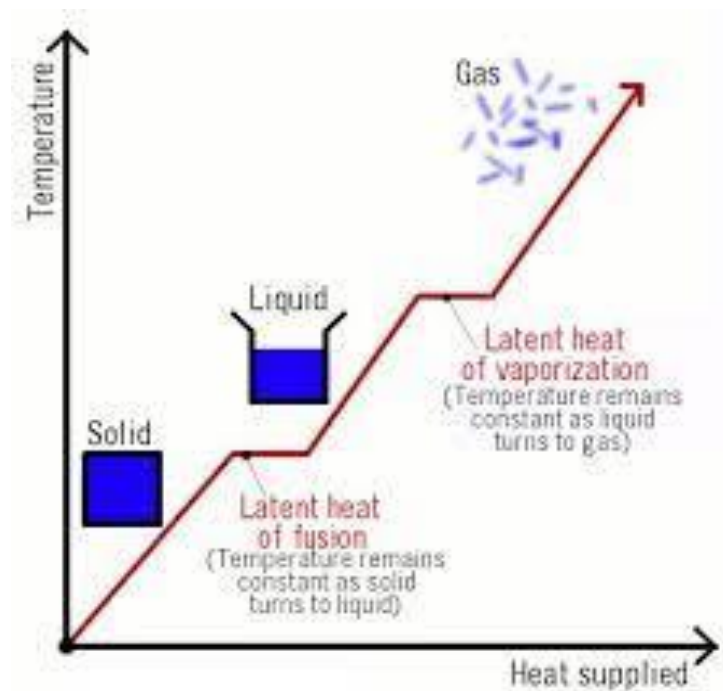


Figure 17. The difference between sensible and latent heat. Sensible heat is the increasing portions of the graph between the plateaus. Sensible heat increases the temperature of the system while latent heat is the heat needed for phase change (plateaus [55]).

Appendix D – TRL levels for EMS

TRL 9

- ThermaBlox is purchasable with the inclusion of EMS

TRL 8

- EMS have been proven in ThermaBlox environment and ready for sale.

TRL 7

- Data gathered from EMS inclusion in pilot plant molten salt loops confirms modeling assumptions and results

TRL 6

- Data from EMS testing in external molten salt loop is satisfactory at high temperature and corrosion levels.

TRL 5

- EMS satisfactorily demonstrates survivability in a high temperature environment

TRL 4

- EMS can be produced at kg-scale in a laboratory environment with satisfactory modeling data based on prototype material properties.

TRL 3

- Models generated based expected formulation verify the potential for EMS inclusion in molten salt loops.

TRL 2

- Cratus believes low energy density thermal energy storage can be solved with the inclusion of EMS.

TRL 1

- Thermal energy storage systems suffer from low comparative energy density.

Bibliography

1. “EIA - U.S. Battery Storage Market Trends.”
<https://www.eia.gov/analysis/studies/electricity/batterystorage/> (accessed May 08, 2022).
2. H. Ritchie and M. Roser, “CO₂ and Greenhouse Gas Emissions,” Our World in Data, May 2020, Accessed: Dec. 12, 2021. [Online]. Available:
<https://ourworldindata.org/co2-emissions>
3. D. Lüthi *et al.*, “High-resolution carbon dioxide concentration record 650,000–800,000 years before present,” *Nature*, vol. 453, no. 7193, pp. 379–382, May 2008, doi: [10.1038/nature06949](https://doi.org/10.1038/nature06949).
4. M. Shellenberger, “Renewable Energy Boom Risks More Blackouts Without Adequate Investment In Grid Reliability,” *Forbes*.
<https://www.forbes.com/sites/michaelshellenberger/2021/04/20/why-renewables-cause-blackouts-and-increase-vulnerability-to-extreme-weather/> (accessed May 03, 2022).
5. March 02 and 2021 Ralph Cavanagh, “A Tale of Two Grids: Texas and California,” NRDC. <https://www.nrdc.org/experts/ralph-cavanagh/tale-two-grids-texas-and-california> (accessed May 08, 2022).
6. “California ISO - Renewables and emissions reports.”
<https://www.caiso.com/market/Pages/ReportsBulletins/RenewablesReporting.aspx> (accessed May 01, 2022).
7. “Confronting the Duck Curve: How to Address Over-Generation of Solar Energy,” Energy.gov. <https://www.energy.gov/eere/articles/confronting-duck-curve-how-address-over-generation-solar-energy> (accessed May 01, 2022).
8. “50060.pdf.” <https://www1.eere.energy.gov/solar/pdfs/50060.pdf> (accessed May 04, 2022).
9. “Rolling Blackouts.” <https://www.directenergy.com/learning-center/rolling-blackouts> (accessed May 04, 2022). “How Does the U.S. Power Grid Work?,” *Council on Foreign Relations*. <https://www.cfr.org/backgrounder/how-does-us-power-grid-work> (accessed Feb. 20, 2022).
10. “How Does the U.S. Power Grid Work?,” *Council on Foreign Relations*.
<https://www.cfr.org/backgrounder/how-does-us-power-grid-work> (accessed Feb. 20, 2022).
11. “How Pumped Storage Hydropower Works,” *Energy.gov*.
<https://www.energy.gov/eere/water/how-pumped-storage-hydropower-works> (accessed Apr. 24, 2022).
12. “Pumped Hydro Storage - The Ups and Downs of Water,” *Alternative Energy Tutorials*. <https://www.alternative-energy-tutorials.com/hydro-energy/pumped-hydro-storage.html> (accessed May 01, 2022).
13. “Utility-scale batteries and pumped storage return about 80% of the electricity they store.” <https://www.eia.gov/todayinenergy/detail.php?id=46756> (accessed Apr. 24, 2022).

14. "Pumped Hydro Moves to Retain Storage Market Leadership."
<https://www.greentechmedia.com/articles/read/pumped-hydro-moves-to-retain-storage-market-leadership> (accessed Apr. 24, 2022).
15. "Hydroelectric power resources form regional clusters."
<https://www.eia.gov/todayinenergy/detail.php?id=1750> (accessed May 01, 2022).
16. "ANU finds 530,000 potential pumped-hydro sites worldwide," *ANU*, Mar. 31, 2019. <https://www.anu.edu.au/news/all-news/anu-finds-530000-potential-pumped-hydro-sites-worldwide> (accessed May 01, 2022).
17. F. Lambert, "Tesla reveals Megapack prices: starts at \$1 million," *Electrek*, Jul. 26, 2021. <https://electrek.co/2021/07/26/tesla-reveals-megapack-prices/> (accessed Apr. 25, 2022).
18. "tsla-10k_20201231.htm."
https://www.sec.gov/Archives/edgar/data/1318605/000156459021004599/tsla-10k_20201231.htm (accessed Apr. 25, 2022).
19. "Technologies," *EASE Storage*. <https://ease-storage.eu/energy-storage/technologies/> (accessed Apr. 28, 2022).
20. S. Tetteh, M. R. Yazdani, and A. Santasalo-Aarnio, "Cost-effective Electro-Thermal Energy Storage to balance small scale renewable energy systems," *Journal of Energy Storage*, vol. 41, p. 102829, Sep. 2021, doi: [10.1016/j.est.2021.102829](https://doi.org/10.1016/j.est.2021.102829).
21. D. Llamas, "The Cost of Solar Power from Abengoa's Arizona CSP Plant with Storage," *HELIOSCSP*. <https://helioscsp.com/the-cost-of-solar-power-from-abengoas-arizona-csp-plant-with-storage/> (accessed May 08, 2022).
22. "A. Madrigal, "New Plant Could Drop Cost of Solar Power to 1.5x US Average," *Wired*. Accessed: May 08, 2022. [Online]. Available: <https://www.wired.com/2008/02/new-plant-could/>
23. M. Amiryar, "A review of flywheel energy storage system technologies and their applications." *Applied Sciences*. <https://www.mdpi.com/2076-3417/7/3/286/pdf>
24. "Comprehensive Energy Systems | ScienceDirect."
<https://www.sciencedirect.com/referencework/9780128149256/comprehensive-energy-systems> (accessed Apr. 30, 2022).
25. "Supercritical CO2." https://www.itec-es.co.jp/English/co2/co2_00.html (accessed Feb. 03, 2022).
26. "Thermal Efficiency Formula | Calculation | nuclear-power.com," *Nuclear Power*. <https://www.nuclear-power.com/nuclear-engineering/thermodynamics/laws-of-thermodynamics/thermal-efficiency/thermal-efficiency-formula/> (accessed May 22, 2022).
27. M. Vick, A. Heyes, and K. Pullen, "Design Overview of a Three Kilowatt Recuperated Ceramic Turbohaft Engine," *Journal of Engineering for Gas Turbines and Power-transactions of The Asme - J ENG GAS TURB POWER-T ASME*, vol. 132, Sep. 2010, doi: [10.1115/1.4000585](https://doi.org/10.1115/1.4000585).

28. "QTR2015-4R-Supercritical-Carbon-Dioxide-Brayton Cycle.pdf."
<https://www.energy.gov/sites/default/files/2016/06/f32/QTR2015-4R-Supercritical-Carbon-Dioxide-Brayton%20Cycle.pdf> (accessed May 01, 2022).
29. E. J. Parma *et al.*, "Supercritical CO₂ Brayton Cycle," p. 28.
30. "UCSB Science Line." <https://scienceline.ucsb.edu/getkey.php?key=563#> (accessed May 08, 2022).
31. T. L. Liu, W. R. Liu, and X. H. Xu, "Properties and heat transfer coefficients of four molten-salt high temperature heat transfer fluid candidates for concentrating solar power plants," *IOP Conf. Ser.: Earth Environ. Sci.*, vol. 93, p. 012023, Nov. 2017, doi: [10.1088/1755-1315/93/1/012023](https://doi.org/10.1088/1755-1315/93/1/012023).
32. Q.-G. Zhao, C.-X. Hu, S.-J. Liu, H. Guo, and Y.-T. Wu, "The thermal conductivity of molten NaNO₃, KNO₃, and their mixtures," *Energy Procedia*, vol. 143, pp. 774–779, Dec. 2017, doi: 10.1016/j.egypro.2017.12.761.
33. R. G. Reddy, "Novel Molten Salts Thermal Energy Storage for Concentrating Solar Power Generation," Technical Report, 1111584, Oct. 2013. doi: [10.2172/1111584](https://doi.org/10.2172/1111584).
34. K. Britsch, M. Anderson, P. Brooks, and K. Sridharan, "Natural circulation FLiBe loop overview," *International Journal of Heat and Mass Transfer*, vol. 134, pp. 970–983, May 2019, doi: [10.1016/j.ijheatmasstransfer.2018.12.180](https://doi.org/10.1016/j.ijheatmasstransfer.2018.12.180).
35. Manohar S. Sohal, Matthias A. Ebner, Piyush Sabharwall, and Phil Sharpe, "Engineering Database of Liquid Salt Thermophysical and Thermochemical Properties," INL/EXT-10-18297, 980801, Mar. 2010. doi: [10.2172/980801](https://doi.org/10.2172/980801).
36. K. Britsch, M. Anderson, P. Brooks, and K. Sridharan, "Natural circulation FLiBe loop overview," *International Journal of Heat and Mass Transfer*, vol. 134, pp. 970–983, May 2019, doi: 10.1016/j.ijheatmasstransfer.2018.12.180.
37. X.-H. An, J.-H. Cheng, H.-Q. Yin, L.-D. Xie, and P. Zhang, "Thermal conductivity of high temperature fluoride molten salt determined by laser flash technique," *International Journal of Heat and Mass Transfer*, vol. 90, pp. 872–877, Nov. 2015, doi: 10.1016/j.ijheatmasstransfer.2015.07.042.
38. P. B. Salunkhe and P. S. Shembekar, "A review on effect of phase change material encapsulation on the thermal performance of a system," *Renewable and Sustainable Energy Reviews*, vol. 16, no. 8, pp. 5603–5616, Oct. 2012, doi: [10.1016/j.rser.2012.05.037](https://doi.org/10.1016/j.rser.2012.05.037).
39. dvgulik, "TECHNOLOGY," *Cratus*. <https://cratus-energy.com/technology/> (accessed May 01, 2022).
40. "Utilisation of waste heat in the steel industry – GMH Gruppe."
<https://www.gmh-gruppe.de/de-en/green-steel/value-stream-increasingly-sustainable/utilisation-of-waste-heat-in-the-steel-industry.html> (accessed May 01, 2022).
41. "Utilisation of waste heat in the steel industry – GMH Gruppe."
<https://www.gmh-gruppe.de/de-en/green-steel/value-stream-increasingly->

- [sustainable/utilisation-of-waste-heat-in-the-steel-industry.html](#) (accessed May 01, 2022).
42. "Iron And Steel Mills And Ferroalloy Manufacturing Global Market Briefing 2020: Covid 19 Impact and Recovery."
<https://www.marketresearch.com/Business-Research-Company-v4006/Iron-Steel-Mills-Ferroalloy-Manufacturing-13832541/> (accessed May 01, 2022).
 43. "2021 bof steelmaking cost model basic oxygen furnace."
<https://www.steelonthenet.com/cost-bof.html> (accessed Apr. 01, 2022).
 44. M. Mohsen and B. Akash, "Energy analysis of the steel making industry," *International Journal of Energy Research*, vol. 22, pp. 1049–1054, Oct. 1998, doi: [10.1002/\(SICI\)1099-114X\(199810\)22:12<1049::AID-ER422>3.3.CO;2-N](https://doi.org/10.1002/(SICI)1099-114X(199810)22:12<1049::AID-ER422>3.3.CO;2-N).
 45. "Energy Department Announces Achievement of SunShot Goal, New Focus for Solar Energy Office," *Energy.gov*. <https://www.energy.gov/articles/energy-department-announces-achievement-sunshot-goal-new-focus-solar-energy-office> (accessed Apr. 30, 2022).
 46. "BCC Library - Report View - EGY165A." <https://academic-bccresearch-com.eu1.proxy.openathens.net/market-research/energy-and-resources/solar-energy-markets.html> (accessed May 01, 2022).
 47. "Innovation outlook: Thermal energy storage,"
/publications/2020/Nov/Innovation-outlook-Thermal-energy-storage.
<https://www.irena.org/publications/2020/Nov/Innovation-outlook-Thermal-energy-storage> (accessed May 01, 2022).
 48. "Generation IV Nuclear Reactors: WNA - World Nuclear Association."
<https://world-nuclear.org/information-library/nuclear-fuel-cycle/nuclear-power-reactors/generation-iv-nuclear-reactors.aspx> (accessed Apr. 30, 2022).
 49. S. Patel, "China Starts Up First Fourth-Generation Nuclear Reactor," *POWER Magazine*, Feb. 01, 2022. <https://www.powermag.com/china-starts-up-first-fourth-generation-nuclear-reactor/> (accessed Apr. 30, 2022).
 50. "BCC Library - Report View - EGY073B." <https://academic-bccresearch-com.eu1.proxy.openathens.net/market-research/energy-and-resources/alternative-power-storage-technologies-report.html> (accessed May 01, 2022).
 51. I. Tzinis, "Technology Readiness Level," NASA, May 06, 2015.
http://www.nasa.gov/directorates/heo/scan/engineering/technology/technology_readiness_level (accessed May 01, 2022).
 52. "2021 CMTS," *Tableau Software*.
<https://public.tableau.com/views/2021CMTS/TechSummary?:embed=y&Technology=Utility-Scale%20Battery%20Storage&:embed=y&:showVizHome=n&:bootstrapWhenNotified=y&:apiID=handler0> (accessed May 01, 2022).

53. P. B. Salunkhe and P. S. Shembekar, "A review on effect of phase change material encapsulation on the thermal performance of a system," *Renewable and Sustainable Energy Reviews*, vol. 16, no. 8, pp. 5603–5616, Oct. 2012, doi: 10.1016/j.rser.2012.05.037.
54. M. Ghiji *et al.*, "A Review of Lithium-Ion Battery Fire Suppression," *Energies*, vol. 13, no. 19, Art. no. 19, Jan. 2020, doi: [10.3390/en13195117](https://doi.org/10.3390/en13195117).
55. "Latent and Sensible Heat | North Carolina Climate Office." <https://legacy.climate.ncsu.edu/edu/Heat> (accessed May 02, 2022).